A NOVEL DUAL-MODE DUAL-FREQUENCY LINAC DESIGN

Mamdouh Nasr*, Sami Tantawi
SLAC National Accelerator Laboratory, CA, USA

Abstract

We present a new type of accelerator structure that operates simultaneously at two accelerating modes with two frequencies. These frequencies are not harmonically related, but rather have a common sub-harmonic. This design will use a recently developed parallel feeding network that feeds every cavity cell independently using a distributed feeding network. We will provide the theoretical background for our dual-mode design as well as our optimization results.

INTRODUCTION

The idea of using multi-mode accelerating cavities have been around for a long time [1]. Also, in the past few years, there have been an effort to utilize multi-mode cavities to enhance the performance of RF electron guns as well as accelerating cavities [2–5]. All this work, however, strict the designs to harmonically related frequencies which is not optimal and even sometimes degrades the performance from that of an optimized single-frequency structures.

In this work, we will design for frequencies that are not necessarily harmonically related, but rather have a common sub-harmonic. We will also utilize a recently developed parallel distributed-feeding network that feeds every cell independently [6]. The main advantage of this feeding technique is that for minimally-coupled cells, the design problem converges to a single cell design which leads to much enhanced efficiency that can easily double the shunt impedance compared to conventionally fed accelerator structures. This idea have been developed and is under testing at SLAC for a single-mode X-band standing wave (SW) linac achieving a shunt impedance of 156 MΩ/m for iris diameter of 0.1λ. Based on this, our design problem will converge to a single-cell design for dual-modes that are not necessarily harmonically related which will lead to much enhanced performance over that of single-mode optimized designs.

CONCEPTUAL FOUNDATION

First, we need to have a better understanding of the dual-mode operation by deriving an expression for the total shunt impedance and the required condition to maximize its value. We can express the total energy gain for a charged particle with a charge (e) that passes on-axis through a cavity of length (L) and operating simultaneously with two modes (with subscripts 1 and 2) as follows:

$$\Delta U = e\int_0^L \mathcal{E}_{tot}(z,t)dz = e\int_0^L \left[\mathcal{E}_1(z,t)+\mathcal{E}_2(z,t)\right]dz = e\left[G_1+G_2\right]L = eG_{tot}L \quad (1)$$

where $\mathcal{E}_{1,2}(z,t)$ and $G_{1,2}$ are the axial electric field and average gradient for each individual mode, respectively; while, G_{tot} is the total gradient for the dual-mode operation.

Using the basic definition of shunt impedance for each mode, we can express the squared total gradient as follows:

$$G_{tot}^2 = (G_1+G_2)^2 = r_1P_{L1} + r_2P_{L2} + 2\sqrt{r_1r_2P_{L1}P_{L2}} \quad (2)$$

where $r_{1,2}$ and $P_{L1,2}$ are the shunt impedance and power loss for each mode operating individually. From this result, we can express the total shunt impedance as follows:

$$r_{tot} = \frac{G_{tot}^2}{P_{Ltot}} = \frac{r_1P_{L1} + r_2P_{L2} + 2\sqrt{r_1r_2P_{L1}P_{L2}}}{P_{L1}+P_{L2}} \quad (3)$$

Now, let's define α as the ratio between power losses of the two modes such that $P_{L2} = \alpha P_{L1}$

$$\therefore r_{tot} = \frac{r_1 + \alpha r_2 + 2\sqrt{\alpha r_1 r_2}}{1+\alpha} \quad (4)$$

The optimal value of α that maximize the total shunt impedance is then derived by equating $\partial r_{tot}/\partial\alpha$ to zero leading to the following results:

$$\alpha_1 = \frac{r_2}{r_1} \rightarrow r_{tot,1} = r_1 + r_2 \quad (5)$$

$$\alpha_2 = \frac{r_1}{r_2} \rightarrow r_{tot,2} = 4\frac{r_1r_2}{r_1+r_2} \quad (6)$$

It can be easily proven that $r_{tot,1}$ is always larger than $r_{tot,2}$, consequently, in order to maximize the shunt impedance α should equal to r_2/r_1

$$\therefore \frac{G_2}{G_1} = \sqrt{\frac{r_2P_{L2}}{r_1P_{L1}}} = \frac{r_2}{r_1} = \frac{P_{L2}}{P_{L1}} \quad (7)$$

From this we should point out two facts. First, that the maximum total shunt impedance for dual-mode operation equals to the summation of the individual shunt impedance for each mode under the constraint that the gradient (power) ratio equals to the individual shunt impedance ratio. Second, the derivation didn't require any harmonic relation between the operating frequencies.

In order to give a feeling of the gain from using dual-mode operation, let's assume first a single-mode operation where increasing the gradient by 30% will result in increasing the power loss by ~70% following the square law relation. However, if instead we kept the power level the same for this mode and operated simultaneously with a second mode with shunt impedance $r_2 = 0.3\,r_1$, the total power loss in the cavity using (7) will increase only by 30% i.e. we saved ~40% increase in the power loss for the same gradient by using dual-modes.

* mamdouh@slac.stanford.edu

OPTIMIZATION RESULTS

In this section, we are presenting the optimization results for SW dual-mode cavities. It should be pointed out that the cavities are not necessarily designed to operate with π-mode for the fundamental mode because, however it is the optimum choice for single-mode designs, it is not necessarily optimal for dual-mode ones. Consequently, we added the cell width as an optimization parameter in all of our designs, the phase advance for each cell and mode will be then adjusted by proper design of the parallel distributed feeding networks. Figure 1, displays the shunt impedance of optimized nose-shaped cavity designs for both single and dual-mode operation. The single frequency designs utilizes (a) C-band frequency at 5.712 GHz and (b) X-band frequency at 11.424 GHz; while the dual-mode frequencies uses the same frequencies for the first mode and a second frequency in (a) X and (b) K-bands. We provide two sets of designs that utilize TM_{011} or TM_{020} as the second mode of operation. The figure shows the large increase in the shunt impedance for dual-mode operation. These results exceeds by far any reported ones for multi-mode designs that is limited to harmonic frequencies operation.

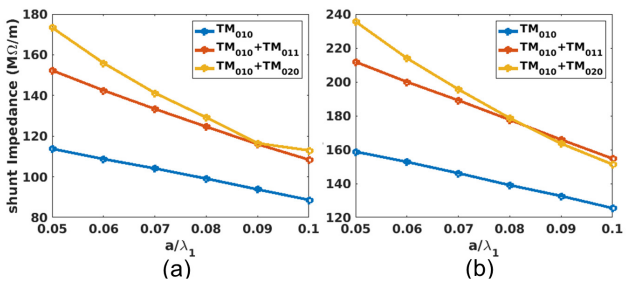

Figure 1: The shunt impedance of optimized designs for both single and dual-mode operation. The single frequency designs utilizes (a) C-band (b) X-band; while the dual frequencies uses the same first mode frequency and a second frequency (TM011 or TM020 mode) in (a) X and (b) K-bands.

It might be useful to point out that the cell width is ~$0.5\lambda_1$ for TM_{010} + TM_{011} designs with $f_{res,2} \approx 1.66 f_{res,1}$, while ~$0.3\lambda_1$ for TM_{010} + TM_{020} designs with $f_{res,2} \approx 2.3 f_{res,1}$. Also, all the designs have maximum surface electric field to gradient ratio of 2.5 where the fields for the second mode in dual-mode operation are scaled by a factor of $\alpha = r_2/r_1$ as described in (7) for optimal operation. In order to have a fair comparison between designs we need to include many factors other than the shunt impedance such as surface magnetic field, power loss into the cavity walls and the S_c-factor [7] that is commonly used to characterize breakdowns. Table 1 provides a detailed comparison of three designs that utilizes single-mode, TM_{010} + TM_{011} modes, and TM_{010} + TM_{020} ones for the same iris diameter of $0.1\lambda_1$ and assuming a total gradient of 100 MV/m.

Table 1 proves the large advantage of dual-mode operation that enhances the accelerator efficiency by the large increase in the shunt impedance as well as an expected enhancement in the cavity breakdown measurements due to the large decrease in the wall losses and the S_c-factor. Also, we can note that TM_{010} + TM_{020} optimized design provides largely enhanced solution even compared to the TM_{010} + TM_{011} one. On the other hand, the wider cells for the latter design is expected to result in a less complicated feeding network design; Also, its operating frequency is in the range of many available medical Klystrons [8,9]. As illustrated in the table, the two solutions can operate with bunch rate up to 163.2 and 380.8 MHz, respectively. The designs can be optimized for even higher common harmonics.

For further illustration Fig. 2 shows the electric field mode plots for the TM_{010} + TM_{011} and TM_{010} + TM_{020} dual-mode designs from Table 1; While Fig. 3 shows the electric and magnetic surface fields plots for the same modes.

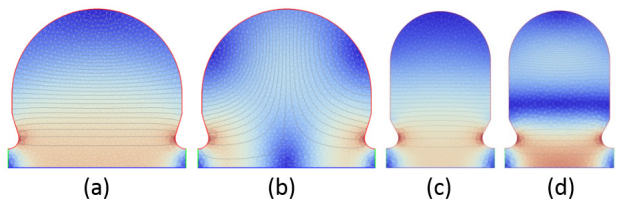

Figure 2: Electric field mode plots for the (a-b)TM_{010}-TM_{011} modes and (c-d) TM_{010}-TM_{020} ones of the designs in Table 1.

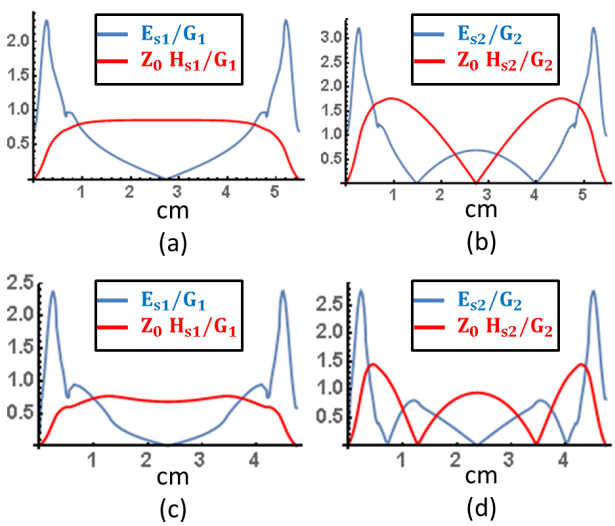

Figure 3: Electric and magnetic surface field mode plots for the (a-b) TM_{010}-TM_{011} modes and (c-d) TM_{010}-TM_{020} ones of the designs Table 1.

Finally, we should mention that all the previous optimizations utilized conventional nose-shaped cavities and yet produced an outstanding performance compared to both single-mode cavities and previously reported multi-mode ones that was strict to harmonically related frequencies. We are now working on developing more optimized generic shapes to

ISBN 978-3-95450-182-3

Table 1: Summary of results for optimized cells with iris diameter of $0.1\lambda_1$ and utilizing single π-mode, TM_{010} + TM_{011} dual-modes, and TM_{010} + TM_{020} ones at a gradient of 100 MV/m

	π-mode	TM_{010} + TM_{011}				TM_{010} + TM_{020}			
	TM_{010}	**1st mode only**	**2nd mode only**	**Dual**		**1st mode only**	**2nd mode only**	**Dual**	
Frequency (GHz)	5.712	5.712	9.6288	-		5.712	12.9472	-	
Common Harmonic (MHz)	-	-	-	163.2		-	-	380.8	
Shunt Impedance (MΩ/m)	113.58	111.0	41.37	152.37	+34.2%	115.4	58.4	173.8	+53%
Max$[E_{surf}]$ (MV/m)	250	230.6	322.5	255.5		236.8	275.1	249.7	
Max$[H_{surf}]$ (MA/m)	0.236	0.228	0.469	0.293	+24.15%	0.203	0.384	0.264	+10.6%
S_c **(W/μm^2)**	5.44	4.33	14.33	3.35	-38.4%	4.3	12.9	3.35	-38.4%
Surface Loss (MW)	2.31	2.28	6.11	1.66	-28.1%	1.273	2.516	0.845	-63.4%

produce even higher performance; Also, we are working on the design for the distributed feeding network for our dual-mode designs.

CONCLUSION

A novel dual-mode designs that utilizes two modes at two different frequencies were introduced. The designs are not constrained to harmonically related frequencies, but rather have a common sub-harmonic. The conceptual foundation was presented illustrating the required constraint to maximum shunt impedance. Also, two set of optimization results were shown for designs operating at C and X-bands and X and K-bands showing the huge gain of using dual-mode operation. Also, two designs utilizing TM_{010} + TM_{011} and TM_{010} + TM_{020} were presented in detail showing both efficiency enhancement as well as predicted decrease in breakdown rate.

REFERENCES

[1] C. E. Hess, H. A. Schwettman, and T. I. Smith, "Harmonically resonant cavities for high brightness beams," *IEEE Transactions on Nuclear Science*, vol. 32, no. 5, pp. 2924–2926, Oct 1985.

[2] J. Lewellen and J. Noonan, "Field-emission cathode gating for rf electron guns," *Physical Review Special Topics-Accelerators and Beams*, vol. 8, no. 3, p. 033502, 2005.

[3] S. V. Kuzikov, A. A. Vikharev, J. L. Hirshfield, Y. Jiang, and V. Vogel, "A Multi-Mode RF Photocathode Gun." 2nd International Particle Accelerator Conference, San Sebastian (Spain), 4 Sep 2011 - 9 Sep 2011. JACoW, Sep 2011. [Online]. Available: http://bib-pubdb1.desy.de/record/91700

[4] Y. Jiang and J. Hirshfield, "Multi-harmonic accelerating cavities for rf breakdown studies," *Proc. of PAC*13, WEPMA28.

[5] S. V. Kuzikov, S. Y. Kazakov, Y. Jiang, and J. L. Hirshfield, "Asymmetric bimodal accelerator cavity for raising rf breakdown thresholds," *Phys. Rev. Lett.*, vol. 104, p. 214801, May 2010. [Online]. Available: https://link.aps.org/doi/10.1103/PhysRevLett.104.214801

[6] S. G. Tantawi, Z. Li, and P. Borchard, "Distributed coupling and multi-frequency microwave accelerators," Jul. 5 2016, uS Patent 9,386,682.

[7] A. Grudiev, S. Calatroni, and W. Wuensch, "New local field quantity describing the high gradient limit of accelerating structures," *Physical Review Special Topics-Accelerators and Beams*, vol. 12, no. 10, p. 102001, 2009.

[8] K. Hayashi, T. Tanaka, K. Hemmi, H. Iyeki, and T. Onodera, "A high power x-band klystron," in *International Technical Digest on Electron Devices Meeting*, Dec 1989, pp. 371–373.

[9] A. Chao and W. Chou, *Reviews of Accelerator Science and Technology: Volume 9: Technology and Applications of Advanced Accelerator Concepts*, 2017. [Online]. Available: https://books.google.com/books?id=Oe-tDgAAQBAJ